*Article*

# Highly Active Non-PGM Catalysts Prepared from Metal Organic Frameworks

**Heather M. Barkholtz** [1,2]**, Lina Chong** [1]**, Zachary B. Kaiser** [1]**, Tao Xu** [2] **and Di-Jia Liu** [1,*]

[1]  Chemical Science and Engineering Division, Argonne National Laboratory, Argonne, IL 60439, USA; E-Mails: barkholtz@anl.gov (H.M.B.); chonglina@anl.gov (L.C.); zkaiser@anl.gov (Z.B.K.)

[2]  Department of Chemistry and Biochemistry, Northern Illinois University, DeKalb, IL 60115, USA; E-Mail: txu@niu.edu

**\*** Author to whom correspondence should be addressed; E-Mail: djliu@anl.gov; Tel./Fax: +1-630-252-4511.

**Abstract:** Finding inexpensive alternatives to platinum group metals (PGMs) is essential for reducing the cost of proton exchange membrane fuel cells (PEMFCs). Numerous materials have been investigated as potential replacements of Pt, of which the transition metal and nitrogen-doped carbon composites ($TM/N_x/C$) prepared from iron doped zeolitic imidazolate frameworks (ZIFs) are among the most active ones in catalyzing the oxygen reduction reaction based on recent studies. In this report, we demonstrate that the catalytic activity of ZIF-based $TM/N_x/C$ composites can be substantially improved through optimization of synthesis and post-treatment processing conditions. Ultimately, oxygen reduction reaction (ORR) electrocatalytic activity must be demonstrated in membrane-electrode assemblies (MEAs) of fuel cells. The process of preparing MEAs using ZIF-based non-PGM electrocatalysts involves many additional factors which may influence the overall catalytic activity at the fuel cell level. Evaluation of parameters such as catalyst loading and perfluorosulfonic acid ionomer to catalyst ratio were optimized. Our overall efforts to optimize both the catalyst and MEA construction process have yielded impressive ORR activity when tested in a fuel cell system.

**Keywords:** non-PGM catalyst; proton exchange membrane fuel cell (PEMFC); oxygen reduction reaction (ORR); zeolitic imidazolate framework (ZIF)

## 1. Introduction

Polymer electrolyte membrane fuel cells are the future powertrain for automotive applications due to their high power density, relatively quick start-up, high efficiency, and emission of only water from the vehicle [1–5]. However, the cathodic oxygen reduction reaction (ORR) kinetics are significantly slower than the anodic hydrogen oxidation reaction [6] therefore requiring more catalyst. To date, the preferred electrocatalysts are platinum or platinum group metals (PGMs), which contribute a significant fraction to the overall fuel cell stack cost [5]. In order for widespread commercialization to take place, technological advancements in cathode catalysts are required, including decreased cost while increasing performance and durability.

The discovery of ORR activity in cobalt phthalocyanine [7] nearly 50 years ago inspired the search for non-PGM ORR electrocatalysts using nitrogen group chelated transition metal complexes, such as metallated phthalocyanines, porphyrins and their analogues, as the precursors of preparing transition metal/nitrogen/carbon ($TM/N_x/C$) catalysts activated via pyrolysis. These precursors typically have square-planar configuration and frequently require high surface area substrates such as amorphous carbons onto which they are supported and dispersed. Using an inert support dilutes the volumetric and gravimetric densities of the possible active sites, limiting the potential of producing highly efficient catalyst. At Argonne National Laboratory, we pioneered the use of zeolitic imidazolate frameworks (ZIFs), a subclass of metal-organic frameworks (MOFs), as precursor templates to prepare ORR electroactive catalysts [8]. MOFs are porous materials comprised organic ligands coordinated to transition metal ions [9,10]. Recently, research surrounding the chemistry and diverse applications of MOF-based materials has experienced tremendous growth [11–14]. For instance, Proietti *et al*. demonstrated that the addition of iron precursors with a Zn-ZIF can give superior fuel cell performance [15]. Since then, several binary ZIF or transition metal doped ZIF systems have been explored as precursors for highly active ORR electrocatalysts [16–19]. For example, we reported an all solid-state one-pot synthesis technique to prepare ZIF based electrocatalysts that demonstrated impressive ORR activity measured by both rotating disk electrode (RDE) and membrane electrode assembly (MEA) in a fuel cell [17].

Our recent study suggests that the catalytic performance of ZIF-based catalysts is very sensitive to the synthesis and processing conditions. In this report, we describe the impact of electrocatalyst processing and MEA fabrication conditions on the overall ORR activity when tested in a single cell fuel cell. We will also discuss how different iron additives could change the fuel cell performance while keeping all other processing parameters the same. Additionally, the influence to fuel cell performance by the addition of small amount of carbon black at different steps of the electrocatalyst synthesis process was investigated. Finally, the weight ratio of Nafion® ionomer to catalyst was optimized in the MEA fabrication process. Overall, an impressive current density of 221.9 mA cm$^{-2}$ at 0.8 V was achieved.

## 2. Results and Discussion

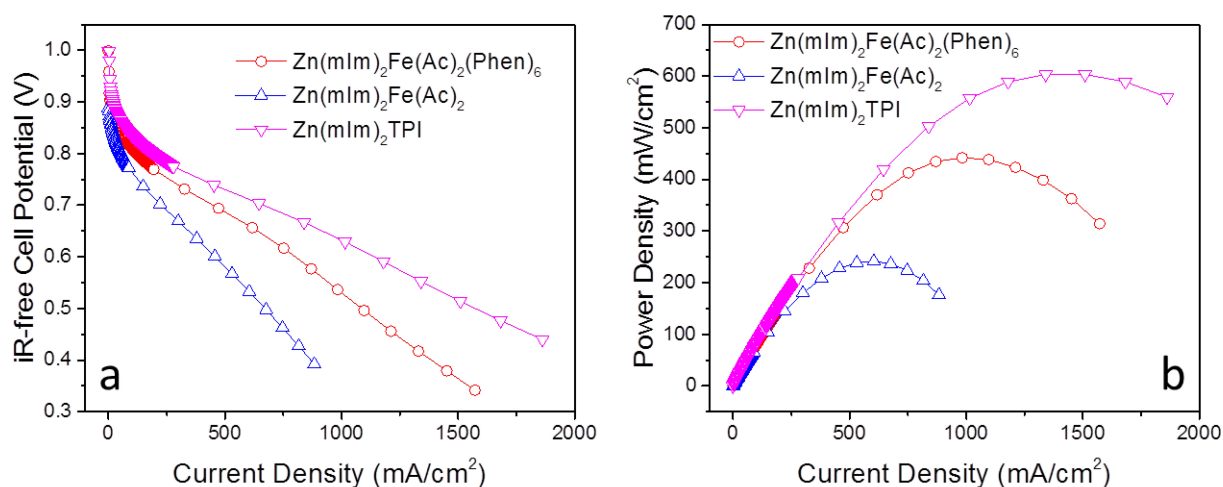### 2.1. Influence of Catalyst Activity by Fe Complex in Precursor

The general procedures for "one-pot" synthesis have been published previously in detail [17]. As a continuation of this study, we investigated the influence of iron precursor and its chelating chemistry to the solid state synthesis and the resulting catalyst performance. In this report, three combinations of iron complexes and organic ligand were applied. They were iron (II) acetate ($Fe(Ac)_2$), tris-1,10-phenanthroline iron (II) perchlorate (TPI) and a combination of iron (II) acetate and 1,10-phenanthroline (Phen) with molar ratio 1:6 ($Fe(Ac)_2(Phen)_6$). For ZIF-8, we used its molecular formula as $Zn(mIm)_2$. The catalyst samples were labeled based on their iron complex and ligand combinations in the $Zn(mIm)_2$ precursor synthesis before the thermal activation. For example, $Zn(mIm)_2Fe(Ac)_2$, represents adding iron acetate directly into mixture for solid state synthesis for $Zn(mIm)_2$. Similarly, $Zn(mIm)_2TPI$ and $Zn(mIm)_2Fe(Ac)_2(Phen)_6$ represent adding TPI and $Fe(Ac)_2$/Phen at 1/6 in the mixtures for solid state synthesis for $Zn(mIm)_2$, respectively. All electrocatalysts underwent normal thermal activation and were fabricated into the cathode of MEAs. The current-voltage polarization and power density curves of the fuel cell tests are shown in Figure 1a,b, respectively. Several key catalyst performance parameters in MEA/fuel cell tests are given by Table 1. It is easily seen that the addition of TPI gave the best overall fuel cell performance. Replacing TPI with $Fe(Ac)_2$ resulted in a 2.5 fold decrease in power density as well as a 3.4 fold decrease in the current density at 0.8 V. Adding in 1,10-phenanthroline as well as iron (II) acetate improved the performance from $Fe(Ac)_2$ but was not equivalent to TPI.

**Table 1.** Brunauer-Emmett-Teller (BET) Surface area and Activity with Different Iron Additives. BET surface area reported on autoclaved samples before any further processing was performed. Fuel cell data is reported for all three samples, including current density at 0.8 $V_{iR-free}$, limiting current, and maximum power density. Fuel cell conditions: $P_{O_2} = P_{H_2} = 1$ bar (back pressure = 7.3 psig) fully humidified; $T = 80$ °C; N211 membrane; 5 $cm^2$ membrane-electrode assemblies (MEA); cathode catalyst = 3.5–4 mg/$cm^2$, anode catalyst = 0.4 $mg_{Pt}$/$cm^2$.

| Sample | BET Surface Area ($m^2$ $g^{-1}$) | Current Density at 0.8 V (mA $cm^{-2}$) | Limiting Current (A $cm^{-2}$) | Power Density (mW $cm^{-2}$) |
|---|---|---|---|---|
| $Zn(mIm)_2Fe(Ac)_2$ | 264.8 | 64.7 | 0.883 | 241.5 |
| $Zn(mIm)_2Fe(Ac)_2(Phen)_6$ | 702.2 | 136.9 | 1.57 | 441.9 |
| $Zn(mIm)_2TPI$ | 859.3 | 221.9 | 1.86 | 603.3 |

We speculate that the Fe-ligand coordination strength plays a very important role in overall electrocatalytic performance. If the iron precursor is able to undergo metal ion exchange with ZIF-8, previous studies have shown that there will be a decrease in fuel cell performance [20]. During the one-pot synthesis, $Fe(Ac)_2$ could be readily dissolved into the liquefied imidazole and water (produced through reaction with zinc oxide) into $Fe^{2+}$ and $Ac^-$. The ionic iron(II) could be incorporated into ZIF framework in the place of $Zn^{2+}$. On the other hand, $Fe^{2+}$ is tightly chelated by six nitrogens from three phenanthroline in an octahedral direction to form a propeller-shaped configuration and will

not readily undergo ion exchange with Zn in Zn(mIm)$_2$ [20]. With significant amounts of Phen present in the iron acetate, imidazole and zinc oxide mixture, it is possible that a certain fraction of Fe$^{2+}$ could ligate with Phen through iron (II)–N bond, as suggested by the previous study [15]. It is difficult, however, to expect that Fe$^{2+}$ will react exclusively with Phen in the presence of excessive amount of imidazole. The consumption of a fraction of available iron (II) to form a Fe-Phen intermediate while the other Fe$^{2+}$ ions chelate with imidazoles as part of ZIF framework may explain the trend seen in Figure 1. Additionally, it is generally accepted that the surface area is an important factor determining fuel cell performance [21]. The Brunauer-Emmett-Teller (BET) surface areas of all three autoclaved catalyst precursors are also given in Table 1. As is shown by the Table, there is a direct correlation between the surface area of the starting material and the overall fuel cell performance. Iron additives in the form of Fe(Ac)$_2$ produced the lowest surface area electrocatalysts therefore the lowest activity, among all three catalysts studied. When Phen was added in addition to Fe(Ac)$_2$, there was a 62.3% increase in precursor surface area, corresponding to a 52.7% increase in the current density at 0.8 $V_{iR-free}$.



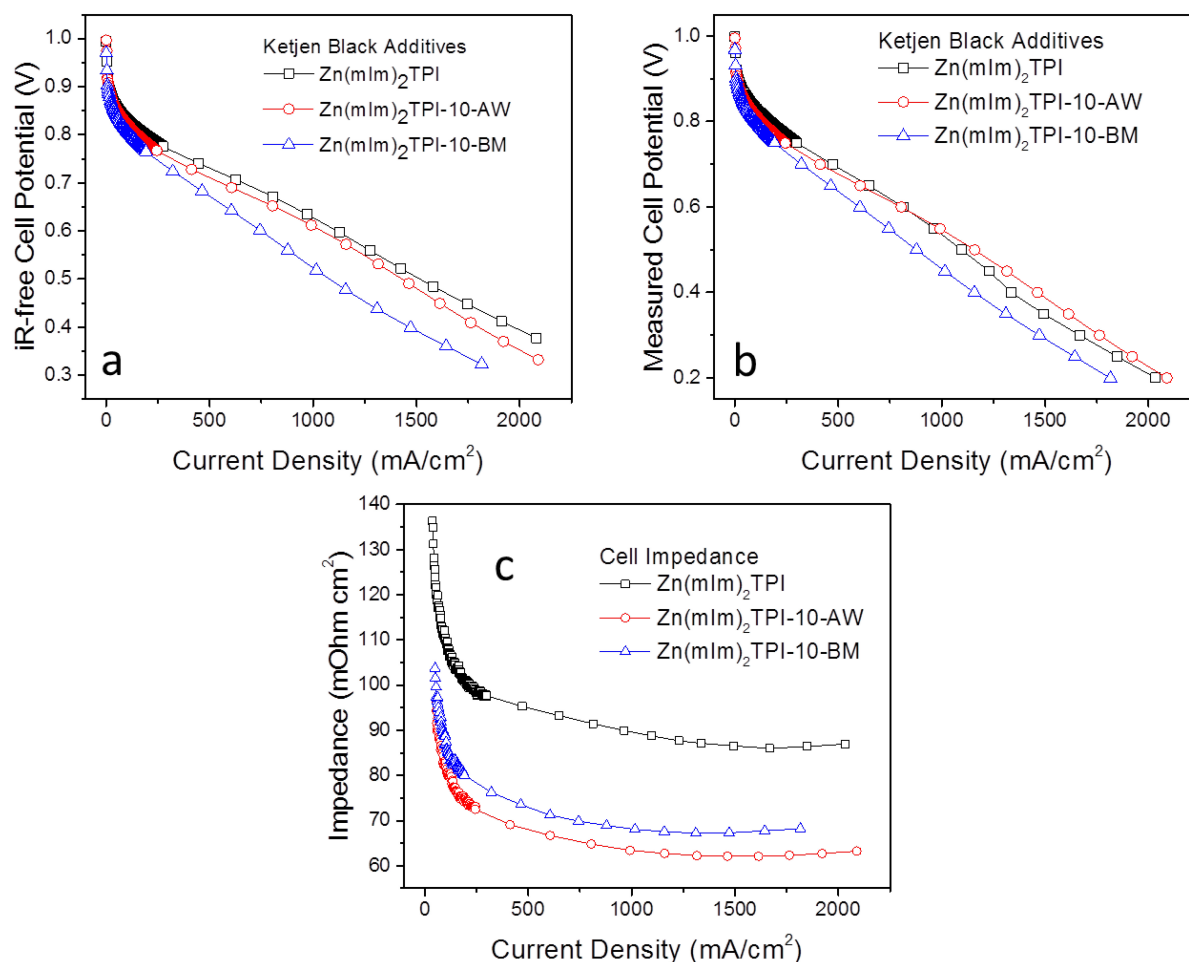**Figure 1.** (**a**) Polarization curves from different iron additive electrocatalysts. The current densities at 0.8 $V_{iR-free}$ for Zn(mIm)$_2$Fe(Ac)$_2$ = 64.7 mA cm$^{-2}$, Zn(mIm)$_2$Fe(Ac)$_2$(Phen)$_6$ = 136.9 mA cm$^{-2}$, and Zn(mIm)$_2$TPI = 221.9 mA cm$^{-2}$. (**b**) Power density curves corresponding to polarization curves shown in (**a**). Maximum power density for Zn(mIm)$_2$Fe(Ac)$_2$ = 241.5 mW cm$^{-2}$, Zn(mIm)$_2$Fe(Ac)$_2$(Phen)$_6$ = 441.9 mW cm$^{-2}$, and Zn(mIm)$_2$TPI = 603.3 mW cm$^{-2}$. Conditions: $P_{O_2} = P_{H_2} = 1$ bar (back pressure = 7.3 psig) fully humidified; $T$ = 80 °C; N211 membrane; 5 cm$^2$ MEA; cathode catalyst = 3.5–4 mg/cm$^2$, anode catalyst = 0.4 mg$_{Pt}$/cm$^2$.

## 2.2. Influence of Adding Carbon Black to MEA Performance

High temperature activation of the ZIF-based precursor converts individual imidazole molecules to graphitic carbon. Such a process often generates incomplete conversion [22], resulting in low electro-conductance of the catalyst and subsequent MEA formed [22]. Mixing a small quantity of carbon black into the heat-activated catalyst could potentially mitigate such an impedance issue. On the other hand, addition of catalytically inert carbon will dilute the ZIF-based catalyst density and

therefore could cause a loss of volumetric and areal specific activities. In this experiment, we selected Ketjen Black as the carbon additive, which is a frequently used carbon support for fuel cell catalysts [23–26]. Two samples were prepared with 10 wt % Ketjen Black EC-300J added at different steps of the electrocatalyst synthesis process. For the first sample, Ketjen Black was added during the ball milling step before thermal activation had occurred. The sample was labeled Zn(mIm)$_2$TPI-10-BM. The second sample was prepared wherein Ketjen Black was added after the thermal activation and acid wash. The sample was labeled Zn(mIm)$_2$TPI-10-AW.



**Figure 2.** (**a**) Impedance corrected polarization curves from Ketjen Black additives and a control sample without any Ketjen Black. (**b**) Polarization curved without impedance correction from Ketjen Black additives and a control sample without any Ketjen Black. (**c**) Cell impedance curves corresponding to polarization curves shown in (**a**) and (**b**). Conditions: $P_{O_2} = P_{H_2} = 1$ bar (back pressure = 7.3 psig) fully humidified; $T = 80$ °C; N211 membrane; 5 cm$^2$ MEA; cathode catalyst = 3.5–4 mg/cm$^2$, anode catalyst = 0.4 mg$_{Pt}$/cm$^2$.

Figure 2a shows the *iR*-free current-voltage polarizations of MEAs with Zn(mIm)$_2$TPI-10-BM and Zn(mIm)$_2$TPI-10-AW as the cathode catalysts, and a MEA without Ketjen Black additive as a benchmark; measured values (without impedance correction) are displayed in Figure 2b. As expected, the cell impedance was reduced by about ~20% for both catalysts containing Ketjen Black additive compared to the benchmark, as is shown in Figure 2c, with Zn(mIm)$_2$TPI-10-AW having
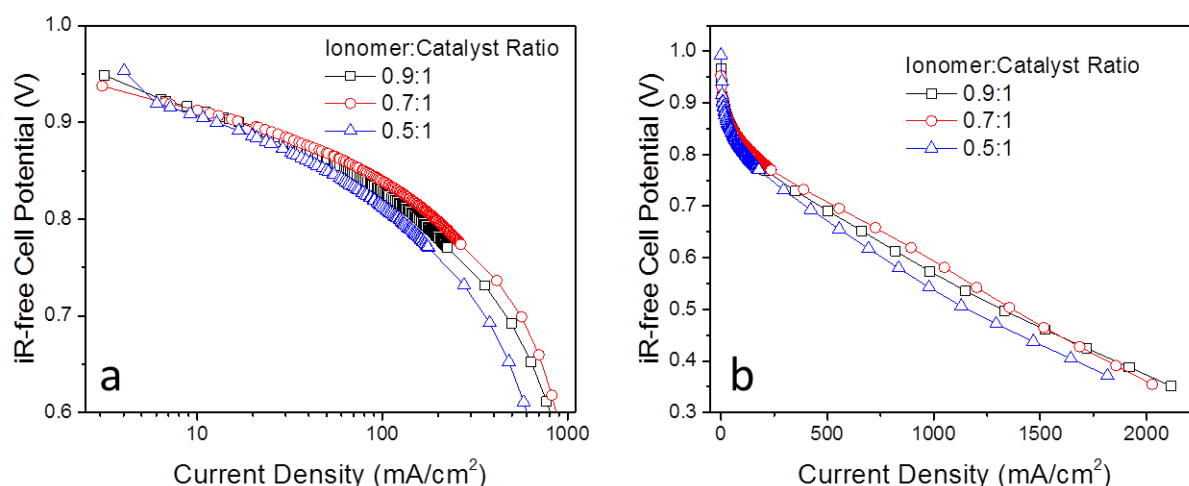
the lowest overall impedance. However, the internal impedance corrected (*iR*-free) polarizations (Figure 2a) show that Zn(mIm)$_2$TPI has the highest fuel cell specific current density among all the samples, suggesting that addition of Ketjen Black causes the dilution of the active sites thereby reducing the overall activity even at a mere 10 wt % loading. Between Zn(mIm)$_2$TPI-10-BM and Zn(mIm)$_2$TPI-10-AW, the latter demonstrates better specific current density at any given cell voltage. Even though both samples contain same amount of Ketjen Black, the amorphous carbon in Zn(mIm)$_2$TPI-10-BM had been subjected to a heat treatment at >1000 °C. Under such temperature, the carbon black would undergo the phase transformation from amorphous to graphitic carbon, accompanied by loss of porosity, volume, and surface area. In contrast, Ketjen Black in Zn(mIm)$_2$TPI-10-AW was added after the high temperature treatment but before the ammonia treatment at 750 °C. The carbon black was still highly porous and more reactive with NH$_3$ for additional active site formation compared to that in Zn(mIm)$_2$TPI-10-BM. Higher catalytic activity is therefore expected. For practical application, the current-voltage polarization without impedance correction represents actual fuel cell performance. Such polarization embodies the balance between the electrode catalyst activity and electron/proton conductivities. To this point, the fuel cell with Zn(mIm)$_2$TPI-10-AW at the cathode offers slightly less desirable performance than Zn(mIm)$_2$TPI at *V* > 0.6 V and slightly better current density at *V* < 0.6 V, see Figure 2b. The cell with Zn(mIm)$_2$TPI-10-BM, however, was inferior over the entire operating region.

*2.3. MEA Fabrication Optimization*

Although the rotating disk electrode (RDE) is the most commonly used method for activity measurements, the electrode catalyst ultimately needs to be measured at MEA/single fuel cell levels since they mostly resemble the operating conditions in a commercial fuel cell stack. Some of the crucial catalyst performance attributes, such as available catalyst area, mass/charge transport efficiencies, triple-phase boundary exposure, *etc.*, will not be properly measured by RDE even though they play extremely important roles in controlling the fuel cell current and power densities. One of the key process parameters for MEA fabrication is the weight ratio between the Nafion$^®$ ionomer and the catalyst. Correct balance between the use and intermixing of ionomer and catalyst could result in optimal exposure of the catalytic active sites and effective proton/electron transfers as well as oxygen and water transports to and from the catalytic sites. This is, in fact, particularly important for our ZIF-derived non-PGM catalysts since their active sites are believed to be uniformly decorated throughout the catalyst surface. We have conducted a series of experiments in MEA optimization by preparing the catalytic ink containing different amount of ionomer and catalyst. The preparation of a cathode catalyst ink includes mixing 5 wt % Nafion$^®$, isopropyl alcohol, water, and thermally activated catalyst. In this experiment, three dry weight ratios between ionomer to the catalyst were applied, from 0.5:1 to 0.9:1.

When optimizing ionomer to catalyst ratios for the ink, it was demonstrated by Figure 3 that 0.7:1 was the optimal ratio to producing the best performing MEA tested in fuel cell. Also noted is that when the ionomer to catalyst ratio was decreased below 0.7:1 to 0.5:1, there was a more discernible drop of cell voltage in both ohmic and limiting-current regions, presumably due to the lack of ion transport caused by insufficient Nafion$^®$. When the ionomer to catalyst ratio was increased to 0.9:1, there was

also an 18.4% decrease in single cell performance at 0.8 $V_{iR\text{-free}}$. This decrease in fuel cell performance may be attributed to excess Nafion® present, clogging the electrocatalyst pores and the electrochemically active surface area, preventing the access of the gas phase oxygen.



**Figure 3.** (**a**) Tafel plots from samples prepared with different ionomer to catalyst ratios. (**b**) Polarization curved corresponding to the Tafel plots shown in (**a**). The current density at 0.8 V for 0.9:1 = 158.4 mA cm$^{-2}$, 0.7:1 = 194.0 mA cm$^{-2}$, and 0.5:1 = 123.5 mA cm$^{-2}$. Conditions: $P_{O_2} = P_{H_2} = 1$ bar (back pressure = 7.3 psig) fully humidified; $T = 80$ °C; N211 membrane; 5 cm$^2$ MEA; cathode catalyst = 3.5–4 mg/cm$^2$, anode catalyst = 0.4 mg$_{Pt}$/cm$^2$.

## 3. Experimental Section

### 3.1. Materials and Methods

Commercially available reagents were used as received without further purification. Ball milling was carried out with a Retsch PM 100 planetary ball mill (Haan, Germany). Fuel cell test stand measurements were carried out on a Scribner 850e fuel cell test stand station (Southern Pines, NC, USA) using a Poco graphite blocks single cell with serpentine flow channels and a geometric electrode surface area of 5 cm$^2$ (Fuel Cell Technology, Albuquerque, NM, USA). The single cell test conditions are given individually under each figure.

### 3.2. One-Pot Synthesis of ZIF-Based Electrocatalyst Precursor

The one-pot synthesis of the ZIF-based electrocatalyst precursor was carried out according to previously reported procedures [17,27]. Preparation of Zn(mIm)$_2$TPI was carried out by adding 2-methylimidazole (668.2 mg, 8 mmol, Aldrich, St. Louis, MO, USA), ZnO (323.5 mg, 4 mmol, Aldrich), and 0.022 mol % iron in the form of 1,10-phenanthroline iron (II) perchlorate (70.5 mg, 0.09 mmol, Aldrich) together, grinding, and sealing in an autoclave under an Ar atmosphere. The autoclave was heated to 180 °C and held for 18 h. A pink powder was obtained and used as described below.

When performing the comparative study, the iron precursor was changed while keeping all other reagents the same as well as the molar percentage of iron added. Two other catalysts were prepared,

$Zn(mIm)_2Fe(Ac)_2$, and $Zn(mIm)_2Fe(Ac)_2(Phen)_6$. Using $Zn(mIm)_2Fe(Ac)_2(Phen)_6$ as an example, the catalyst was prepared by adding 2-methylimidazole (668.2 mg, 8 mmol, Aldrich), ZnO (323.5 mg, 4 mmol, Aldrich), iron (II) acetate (15.6 mg, 0.09 mmol, Aldrich), and 1, 10-phenanthroline (97.3 mg, 0.05 mmol, Aldrich) together, grinding, and sealing in an autoclave under Ar atmosphere. Heating profiles were not changed from what is described above.

### 3.3. Preparation of Electrocatalyst

Pyrolysis of ZIF-based electrocatalyst precursor was carried out by placing about 250 mg of ball milled $Zn(mIm)_2TPI$ into a ceramic boat and inserting it into a quartz tube (2 inch diameter). The tube was sealed and purged with Ar for one hour before it was heated to 1050 °C and held for one hour under flowing Ar atmosphere. The pyrolyzed sample was then acid washed in 0.5 M $H_2SO_4$ via sonication for 30 min then continuously agitated for 16 h at room temperature. The sample was then washed with water until neutral and dried in a vacuum oven at 40 °C. The sample was then pyrolyzed again at 750 °C for 30 min under flowing $NH_3$ atmosphere to give the final product.

When electrocatalysts with Ketjen Black additive were prepared, 10 wt % Ketjen Black was added during either at the ball mill step or after the acid wash and before $NH_3$ thermal activation. As an example, the preparation is given below for $Zn(mIm)_2TPI$-10-AW, where Ketjen Black (4 mg, EC-300J, Azko Nobel, Willowbrook, IL, USA) was added to the electrocatalyst (33.1 mg) after acid wash but before $NH_3$ thermal activation. The sample was dispersed in isopropyl alcohol via sonication for 30 min the dried in a vacuum oven. Once dry, the prepared $Zn(mIm)_2TPI$-10-AW sample was thermally activated at 750 °C for 30 min under $NH_3$ flow per usual.

### 3.4. Single Fuel Cell Test

#### 3.4.1. Preparation of Cathode

An ink solution was prepared for the molar ratio of 0.7:1 ionomer to catalyst by combining $Zn(mIm)_2TPI$ (25 mg) with Nafion® (350 mg, 5 wt. % solution, Aldrich), isopropyl alcohol (890 μL), and water (350 μL). The ink solution was sonicated for 30 min and constantly agitated for 16 h at room temperature before it was painted onto carbon paper (5 cm$^2$, Fuel Cells Etc., Sigracet 25 BC, College Station, TX, USA) to create the cathode, which was dried in a vacuum oven at 40 °C for two hours. The catalyst loading for all the tests was approximately 3.5–4.0 mg cm$^{-2}$.

#### 3.4.2. Preparation of Anode

An ink solution was prepared by combining Pt/C (10 mg, 40 wt. % of Pt, E-TEK, Somerset, NJ, USA), Nafion® (80 mg, 5 wt. % solution, Aldrich), isopropyl alcohol (205 μL), and water (80 μL). This ink solution was solicited for 30 min and constantly agitated for 16 h at room temperature before it was painted onto carbon paper (5 cm$^2$, Fuel Cells Etc., Sigracet 25 BC) to create the anode, which was dried in a vacuum oven at 40 °C for 2 h. The Pt loading for all tests was approximately 0.4 mg$_{Pt}$/cm$^2$.

### 3.4.3. Preparation of Membrane Electrode Assembly

The prepared cathode and anode were hot pressed on either side of a Nafion® N211 membrane (DuPont, New Castle, DE, USA) at 120 °C for 30 s using a pressure of $5.4 \times 10^6$ Pa, the pressure was then increased to $1.1 \times 10^7$ Pa and held for an additional 30 s. Pressure values were calculated assuming that the load is evenly applied to the 5 cm$^2$ electrode.

### 3.4.4. Fuel Cell Activity Test

Fuel cell activity tests were carried out by placing the prepared MEA into a single cell. Data was gathered by a Scribner 850e fuel cell test stand. A polarization curve was recorded by scanning from open circuit potential (OCV) to 750 mV at 10 mA s$^{-1}$ then from 750 mV to 200 mV at 50 mV s$^{-1}$. The area current density, $I_A$, was recorded directly from the polarization measurement. Cell impedance was measured by the current interrupt method installed in the fuel cell test stand.

## 4. Conclusions

Our study shows that significant improvements in cathodic electrocatalyst performance can be achieved when synthesis, processing, and fabrication parameters are optimized. We found that iron complex with six-*N* coordination such as 1,10-phenanthroline iron (II) perchlorate could provide excellent catalytic activity and overall single cell performance. Amorphous carbon such as Ketjen Black was also added at different steps of catalyst preparation to reduce the cell impedance. However, such addition also dilutes the catalytically active sites and thereby reduced the fuel cell performance. Finally, different Nafion® to catalyst ratios were used to improve the cathode ink formulation before MEA fabrication was performed. These improvements at both catalyst and MEA levels have yielded impressive ORR activity when tested in a fuel cell system, moving towards the performance targets set by the U.S. DOE for the automotive application.

## Author Contributions

HMB prepared the samples, performed the experiment and wrote manuscript. LC and ZBK supported the experiments. TX supervised HMB and DJL designed and oversaw the experiment and manuscript preparation.

## Conflicts of Interest

The authors declare no conflict of interest.

## References

1. Costamagna, P.; Srinivasan, S. Quantum jumps in the pemfc science and technology from the 1960s to the year 2000 part ii. Engineering, technology development and application aspects. *J. Power Sources* **2001**, *102*, 253–269.

2. Debe, M.K. Electrocatalyst approaches and challenges for automotive fuel cells. *Nature* **2012**, *486*, 43–51.

3. Mehta, V.; Cooper, J.S. Review and analysis of pem fuel cell design and manufacturing. *J. Power Sources* **2003**, *114*, 32–53.

4. Wagner, F.T.; Lakshmanan, B.; Mathias, M.F. Electrochemistry and the future of the automobile. *J. Phys. Chem. Lett.* **2010**, *1*, 2204–2219.

5. Wong, W.Y.; Daud, W.R.W.; Mohamad, A.B.; Kadhum, A.A.H.; Loh, K.S.; Majlan, E.H. Recent progress in nitrogen-doped carbon and its composites as electrocatalysts for fuel cell applications. *Int. J. Hydrogen Energ.* **2013**, *38*, 9370–9386.

6. Gewirth, A.A.; Thorum, M.S. Electroreduction of dioxygen for fuel-cell applications: Materials and challenges. *Inorg. Chem.* **2010**, *49*, 3557–3566.

7. Jasinski, R. A new fuel cell cathode catalyst. *Nature* **1964**, *201*, 1212–1213.

8. Ma, S.Q.; Goenaga, G.A.; Call, A.V.; Liu, D.J. Cobalt imidazolate framework as precursor for oxygen reduction reaction electrocatalysts. *Chem. Eur. J.* **2011**, *17*, 2063–2067.

9. Carne, A.; Carbonell, C.; Imaz, I.; Maspoch, D. Nanoscale metal-organic materials. *Chem. Soc. Rev.* **2011**, *40*, 291–305.

10. James, S.L. Metal-organic frameworks. *Chem. Soc. Rev.* **2003**, *32*, 276–288.

11. Allendorf, M.D.; Schwartzberg, A.; Stavila, V.; Talin, A.A. A roadmap to implementing metal-organic frameworks in electronic devices: Challenges and critical directions. *Chem. Eur. J.* **2011**, *17*, 11372–11388.

12. Ariga, K.; Yamauchi, Y.; Rydzek, G.; Ji, Q.M.; Yonamine, Y.; Wu, K.C.W.; Hill, J.P. Layer-by-layer nanoarchitectonics: Invention, innovation, and evolution. *Chem. Lett.* **2014**, *43*, 36–68.

13. Gascon, J.; Corma, A.; Kapteijn, F.; Xamena, F.X.L.I. Metal organic framework catalysis: Quo vadis? *ACS Catal.* **2014**, *4*, 361–378.

14. Ryder, M.R.; Tan, J.C. Nanoporous metal organic framework materials for smart applications. *Mater. Sci. Technol.* **2014**, *30*, 1598–1612.

15. Proietti, E.; Jaouen, F.; Lefevre, M.; Larouche, N.; Tian, J.; Herranz, J.; Dodelet, J.P. Iron-based cathode catalyst with enhanced power density in polymer electrolyte membrane fuel cells. *Nat. Commun.* **2011**, *2*, doi:10.1038/ncomms1427.

16. Zhao, D.; Shui, J.L.; Chen, C.; Chen, X.Q.; Reprogle, B.M.; Wang, D.P.; Liu, D.J. Iron imidazolate framework as precursor for electrocatalysts in polymer electrolyte membrane fuel cells. *Chem. Sci.* **2012**, *3*, 3200–3205.

17. Zhao, D.; Shui, J.L.; Grabstanowicz, L.R.; Chen, C.; Commet, S.M.; Xu, T.; Lu, J.; Liu, D.J. Highly efficient non-precious metal electrocatalysts prepared from one-pot synthesized zeolitic imidazolate frameworks. *Adv. Mater.* **2014**, *26*, 1093–1097.

18. Xia, W.; Zhu, J.H.; Guo, W.H.; An, L.; Xia, D.G.; Zou, R.Q. Well-defined carbon polyhedrons prepared from nano metal-organic frameworks for oxygen reduction. *J. Mater. Chem. A* **2014**, *2*, 11606–11613.

19. Zhao, S.L.; Yin, H.J.; Du, L.; He, L.C.; Zhao, K.; Chang, L.; Yin, G.P.; Zhao, H.J.; Liu, S.Q.; Tang, Z.Y. Carbonized nanoscale metal-organic frameworks as high performance electrocatalyst for oxygen reduction reaction. *ACS Nano* **2014**, *8*, 12660–12668.

20. Tian, J.; Morozan, A.; Sougrati, M.T.; Lefevre, M.; Chenitz, R.; Dodelet, J.P.; Jones, D.; Jaouen, F. Optimized synthesis of Fe/N/C cathode catalysts for pem fuel cells: A matter of iron-ligand coordination strength. *Angew. Chem. Int. Edit.* **2013**, *52*, 6867–6870.

21. Jaouen, F.; Herranz, J.; Lefevre, M.; Dodelet, J.P.; Kramm, U.I.; Herrmann, I.; Bogdanoff, P.; Maruyama, J.; Nagaoka, T.; Garsuch, A.; *et al.* Cross-laboratory experimental study of non-noble-metal electrocatalysts for the oxygen reduction reaction. *ACS Appl. Mater. Inter.* **2009**, *1*, 1623–1639.

22. Mikhailenko, S.D.; Afsahi, F.; Kaliaguine, S. Complex impedance spectroscopy study of the thermolysis products of metal-organic frameworks. *J. Phys. Chem. C* **2014**, *118*, 9165–9175.

23. Inoue, H.; Hosoya, K.; Kannari, N.; Ozaki, J. Influence of heat-treatment of ketjen black on the oxygen reduction reaction of Pt/C catalysts. *J. Power Sources* **2012**, *220*, 173–179.

24. Lee, J.S.; Park, G.S.; Kim, S.T.; Liu, M.L.; Cho, J. A highly efficient electrocatalyst for the oxygen reduction reaction: N-doped ketjenblack incorporated into Fe/Fe$_3$C-functionalized melamine foam. *Angew. Chem. Int. Edit.* **2013**, *52*, 1026–1030.

25. Nam, G.; Park, J.; Kim, S.T.; Shin, D.B.; Park, N.; Kim, Y.; Lee, J.S.; Cho, J. Metal-free ketjenblack incorporated nitrogen-doped carbon sheets derived from gelatin as oxygen reduction catalysts. *Nano Lett.* **2014**, *14*, 1870–1876.

26. Yu, J.R.; Islam, M.N.; Matsuura, T.; Tamano, M.; Hayashi, Y.; Hori, M. Improving the performance of a PEMFC with Ketjenblack EC-600JD carbon black as the material of the microporous layer. *Electrochem. Solid-State Lett.* **2005**, *8*, A320–A323.

27. Lin, J.B.; Lin, R.B.; Cheng, X.N.; Zhang, J.P.; Chen, X.M. Solvent/additive-free synthesis of porous/zeolitic metal azolate frameworks from metal oxide/hydroxide. *Chem. Commun.* **2011**, *47*, 9185–9187.